IPG 2023
INTERNATIONAL PIPELINE GEOTECHNICAL CONFERENCE
November 23rd - 24th. Bogotá D.C. - Colombia
Under the auspices of: arpel
Organize: C-IPG ACIEM
6TH INTERNATIONAL PIPELINE GEOTECHNICAL CONFERENCE IPG 2023

IPG2023-0048

LANDSLIDE HAZARD ASSESSMENT: TOPOLOBAMPO GAS PIPELINE (MEXICO)

Alexandra Montes[1], Sebastián Giraldo[2], Érika Valle[3], Mauro Niño[4]

[1]TC Energy, Calgary, Canadá
[2]SÍSÉ Salud Estructural, CDMX, México
[3] TC Energía, CDMX, México
[4]AON-ERN, CDMX, México

ABSTRACT

This paper presents a practical application of the hazard assessment for landslides triggered by rain and earthquakes. The Topolobampo natural gas pipeline, located across the states of Chihuahua and Sinaloa, Mexico, was selected as a case study. This system is 572 km long, consists of a 30" pipeline and has a capacity of 670 million cubic feet per day. Landslide analyses were performed in accordance with the procedures outlined in [**1**], [**2**], which consider soil properties (e.g. friction angle, cohesion, slope angle, and depth of the sliding layer, among others) and the rate of occurrence of triggering events. These methodologies offer correct characterization of the phenomena since they are analyzed under a probabilistic approach. The results of these evaluations allowed the identification of zones of interest along the pipeline, which corresponded with zones previously identified during construction or operations activities.

Keywords: geohazard, integrity, gas pipeline, earthquake, rainfall, flooding, landslide, probability, GIS, return period

NOMENCLATURE

Q_c	Critical precipitation
Q_{max}	Maximum precipitation
a_c	Critical acceleration
a_{max}	Maximum acceleration
FS	Factor of safety
CEM	Continuo de Elevaciones Mexicano
CENAPRED	Centro Nacional de Prevención de Desastres
CFE	Comisión Federal de Electricidad
CHIRPS	Climate Hazards Group Infrared Precipitation with Station Data
CMORPH-BLD	Climate Prediction Center Morphing Blended Technique
CONAGUA	Comisión Nacional del Agua
GHCN	Global Historical Climatology Network
HydroSHEDS	Hydrological data and maps based on SHuttle Elevation Derivatives at multiple Scales
DEM	Digital Elevation Model
PGA	Peak Ground Acceleration
MRP	Mass removal processes
QM	Quantile Mapping
GIS	Geographical Information System
SRTM	Shuttle Radar Topography Mission
SSN	Servicio Sismológico Nacional
CE	Characteristic earthquake
UCSB	Universidad de California, Santa Bárbara
USGS	U.S. Geological Survey

1. INTRODUCTION

Natural gas transportation is essential for energy generation processes in any country. Therefore, gas pipelines must be designed, built, and operated in compliance with the highest quality and safety standards. Proper gas pipeline maintenance activities during the operational stage guarantees protection not only the infrastructure, but also the community and the environment. Integrity programs define the required activities throughout the operational life of the assets, to manage threats that may cause pipeline damage or failure. The following information is part of the initial studies carried out to identify natural hazards that may exist along the pipeline. Within them, only the landslide assessment will be considered here. Since there are many factors that can trigger the occurrence of a landslide, this paper addresses the landslide hazard assessment triggered by hydrological and seismic conditions.

The models presented here were obtained through a probabilistic methodology, using the information contained in existing databases, which allows identification of areas of interest related to geohazards. It is important to mention that the scope of this document does not include the direct impact that a landslide would have on the pipeline which requires use of other pipeline integrity analysis methodologies.

2. MATERIALS AND METHODS

Following sections contain general description of the natural gas pipeline system and integrity program, the geotechnical and hydrological conditions of the area, as well as the methodologies used in the landslide hazard assessment.

2.1 Gas Pipeline System

The Topolobampo natural gas pipeline is located in the northwest of the Mexican Republic (**FIGURE 1**). It was constructed between 2012 and 2017 and started service in 2018. It connects the states of Chihuahua and Sinaloa, supplying natural gas from the United States to energy demand centers along the Mexican Pacific coast. The pipeline consists of 572 km of 30" diameter pipe and has a capacity of 670 million cubic feet per day.

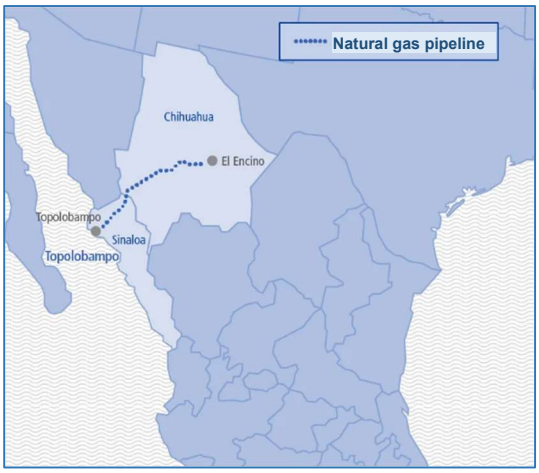

FIGURE 1: LOCATION OF TOPOLOBAMPO GAS PIPELINE *[3]*

The results and methodologies presented in this document are part of the geohazard identification assessment conducted during the operation and maintenance stage, as part of the Topolobampo gas pipeline integrity program.

2.2 Site description

The Topolobampo natural gas pipeline crosses Chihuahua and Sinaloa states, which include several geological, geomorphological, and hydrological characteristics. The identification of these characteristics plays an important role during the entire pipeline life cycle.

Geotechnical and hydrology studies were carried out along the pipeline path, as part of the project engineering design and were used to establish the proper design and construction processes to install the pipe. The following information was taken from these studies and used in the assessment presented in this paper:

- Geological and geotechnical conditions along the gas pipeline
- Seismic zone
- Precipitation levels
- High slope zones
- Landslide zones
- Water body crossings

Based on these studies, about 100 geotechnical boreholes shown in **FIGURE 2** were used to obtain specific soil information such as: volumetric weight, friction angle, cohesion, moisture, stratigraphic profile and granulometry.

FIGURE 2: GEOTECHNICAL BOREHOLES ALONG THE PIPELINE

A spatial interpolation process was applied to this data to create continuous raster files representing the following soil properties along the pipeline:

- Angle of internal friction
- Cohesion
- Volumetric weight
- Moisture content
- Soil profile

Additionally, a Digital Elevation Model (DEM) was created using a LiDAR survey performed by TC Energy, and other sources of information including the *Continuo de Elevaciones Mexicano* (CEM) of INEGI, HydroSHEDS [**4**] and SRTM [**5**]. The resulting DEM with variable resolution is presented in **FIGURE 3**. For this activity, an open-source SIG software was used, QGIS [**6**].

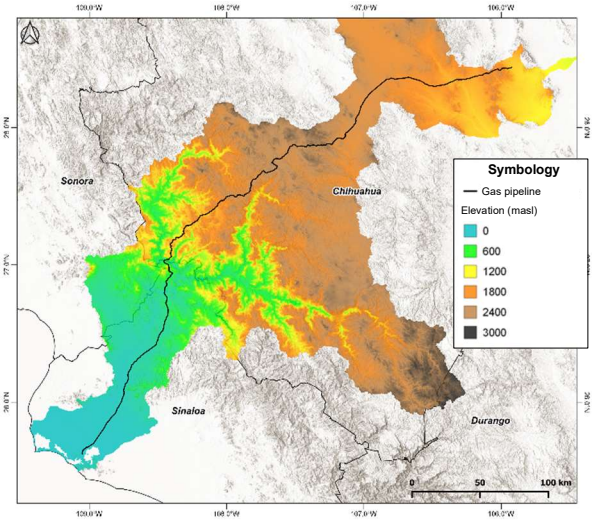

FIGURE 3: DIGITAL ELEVATION MODEL (DEM)

2.3 Pipeline Integrity Program

The identification and management of geotechnical and hydrotechnical hazards, are part of the TC Energy integrity program, the main objective of which is to ensure the continuous and safety operation of the pipeline. The integrity program manages the threats that represent a risk for the operation of the pipeline, which can include:

- Internal and external corrosion
- Cracking
- Manufacturing, design, and construction defects
- Damage by third parties
- Natural hazards
- Incorrect operations

Proper threat identification, evaluation, integrity assessment, and mitigation activities are part of the integrity program and are supported by the inspection and maintenance activities along the pipeline.

Within the realm of natural hazards, geotechnical and hydrotechnical phenomenon that could represent a danger and can impact the pipeline, are considered. For the specific case of Topolobampo pipeline, the geotechnical and hydrotechnical hazards identified along the pipeline included:

- Earthquake
- Landslides
- Subsidence
- Liquefaction
- Geological faults
- Karsticity
- Expansive and collapsible soils
- Floodings
- Scour

For each phenomenon, the presence and or occurrence along the pipeline was determined, using the information available in different resources, such as:

- Centro Nacional de Prevención de Desastres (CENAPRED)
- Risk Atlas of the States of Chihuahua and Sinaloa
- INEGI
- Servicio Geológico Mexicano
- Servicio Sismológico Nacional (SSN)
- Comisión Nacional del Agua (CONAGUA)
- Comisión Federal de Electricidad (CFE)
- Site-specific studies as part of project development (TC Energía)

Each hazard was classified according to TC Energy hazard classification and weather and outside forces threat management program [**7**] that enables prioritize hazard locations and areas of interest.

In this specific case, only identification and evaluation for landslides triggered by earthquakes and rainfall, using the methodology developed by [**1**], [**2**], were addressed. To this end, each triggering phenomenon (precipitation and earthquake) was correctly characterized, and then carried out a probabilistic evaluation of the landslide hazard.

2.4 Trigger Events Characterization

The following sections describe, in general terms, the process followed to characterize the two triggering phenomena under study.

2.4.1 Precipitation

The total precipitation in the hydrological region where the pipeline is located, was determined based on the calculation of the existing runoff that can generate a flood in the land adjacent to the pipeline. A rainfall-runoff model of distributed parameters was created to determine the runoffs from the precipitation.

The Topolobampo pipeline crosses the hydrological regions of Sinaloa, Bravo Conchos and Cuencas Cerradas, numbered 10, 24 and 34, respectively as shown in **FIGURE 4**. In the case of Chihuahua, the gas pipeline section crosses an area with a sub-humid temperate climate, average annual temperature of 17°C with low rainfall during the summer and around 500 mm per year. For Sinaloa area the pipeline crosses zones with a warm subhumid, dry and semi-dry climate with average temperatures

around 25°C. Rainfall occurs in summer with an average annual precipitation of 790 mm per year. The study area was determined according to the sub-basins that have contributions to the watercourses that cross the pipeline (**FIGURE 4**) resulting in a total basin area of 52,221.24 km^2.

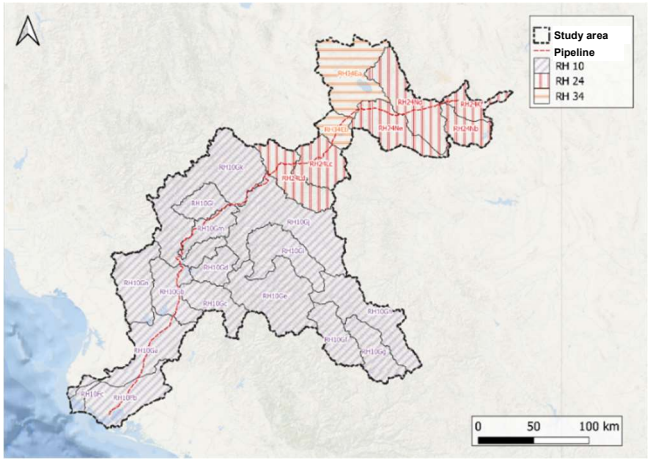

FIGURE 4: PIPELINE HYDROLOGICAL REGIONS

A large part of the pipeline crosses the Sierra Madre Occidental, Mexico's longest mountain system with altitudes ranging from 2000 to 2500 meters above sea level. Based on the cartographic series of vector data for land use and vegetation from *Instituto Nacional de Estadística y Geografía* (INEGI) – *Serie VI Conjunto Nacional,* scale 1:250000 edition 2017, the main vegetation is forest, followed by rainfed agriculture and irrigated agriculture (**FIGURE 5**).

The climate models use to estimate total precipitation employ climate data bases of the Global Historical Climatology Network (GHCN), Climate Hazards Group Infrared Precipitation with Station Data (CHIRPS) and Climate Prediction Center Morphing Blended Technique (CMORPH-BLD).

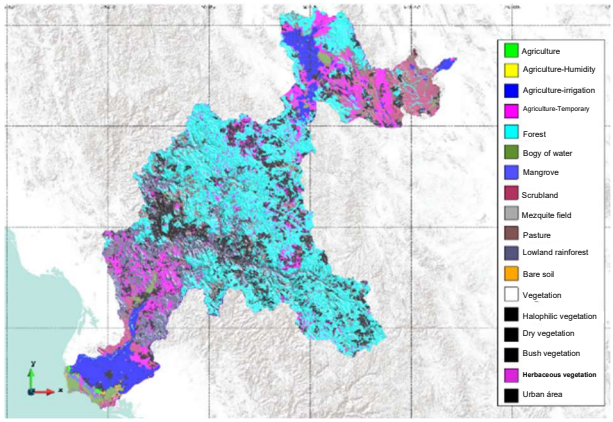

FIGURE 5: PIPELINE LAND USE SPATIAL DISTRIBUTION

Within the study area there are 111 stations belonging to the database GHCN (**FIGURE 6**) of which 47 contain more than 70% of the data. The data from these 47 stations was used for precipitation grids correction.

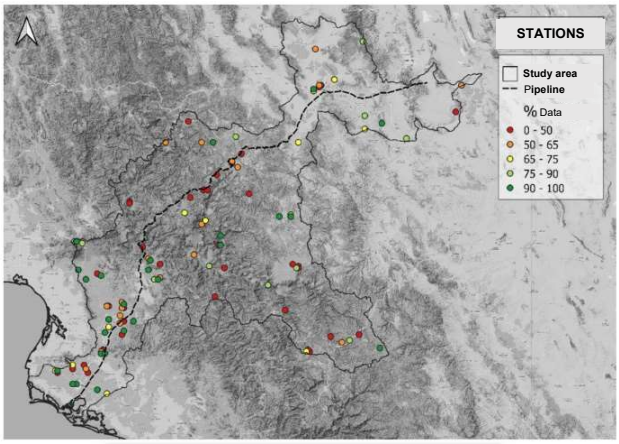

FIGURE 6: STATIONS WITHIN PIPELINE AREA AND % DATA

With the information from the climate databases and using probabilistic models, monthly daily precipitation grids, monthly daily standard deviation grids, and maximum annual precipitation values for return periods[1] of 2, 5, 10, 25, 50, 50, 100, 250 and 500 years were obtained. These calculations were executed using a proprietary code developed in Visual Basic .NET [**8**] that integrates routines already available in the literature. As an example, the precipitation associated with a 100-year return period is presented in the **FIGURE 7**.

The southwestern region of the study area shows the highest precipitation levels for each return periods calculated, which corresponds with the very warm semi-dry climate. This is mainly due to the topographic characteristics with mountainous and

[1] **Return period:** the average period of time that elapses between the occurrence of events of a certain intensity.

coastal areas that promote the entry of humid air to the land, which generates rain in the mountains.

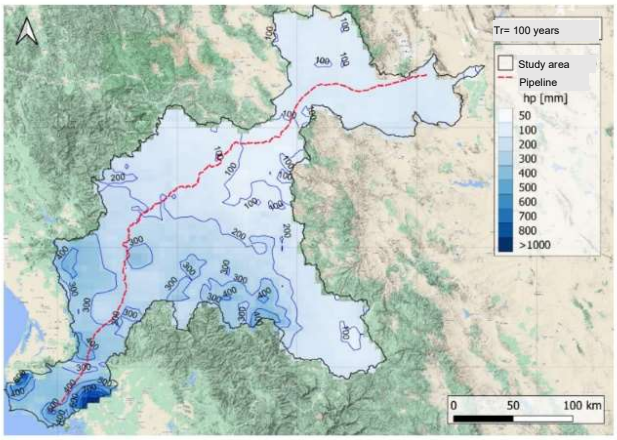

FIGURE 7: PRECIPITATION FOR 100 YEARS RETURN PERIOD

Both the mean and standard deviation reflect the rainfall patterns regime in the study area with variations and higher values between the months of July and September. The precipitation highest values in the study area are located in the mountainous and coastal region (center and southwest), corresponding to the occurrence of torrential and extraordinary rains; while in the northeastern area very heavy and intense rainfall were observed, according to existing information in the National Meteorological Service.

2.4.2 Earthquake

Mexico is one of the most seismically active countries in the world. According to statistical data, more than 90 earthquakes with a magnitude greater than 4 are registered every year, which is equivalent to 6 percent of all the earthquakes registered in the world. **FIGURE 8** shows the zones where most earthquakes occur in Mexico.

Large earthquakes in Mexico (VII to X in MMIS[2]) along the Pacific coast are caused by the subduction of the Cocos and Rivera oceanic plates under the North American plate and are therefore known as subduction earthquakes.

Important events (V to VIII in MMIS[2]) also occur on the continent at depths close to 60 km. In this case the earthquakes present a normal faulting mechanism that reflects the rupture of the subducted oceanic lithosphere [**9**]. Although this type of events occurs less frequently than subduction-type events, it is capable of causing significant damage.

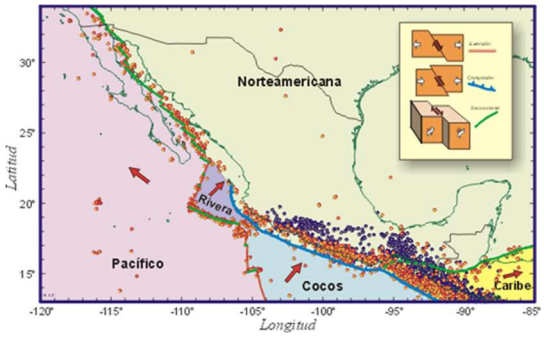

FIGURE 8: TECTONICS, SEISMIC SOURCES AND EPICENTERS IN MEXICO

Even less frequent are earthquakes occurring within the continental plate (IV to VII in MMIS[2]). Depending on their location, such events can generate considerable damage to various human settlements. In Mexico, the Neovolcanic Axis is not parallel to the trench. This is somewhat abnormal compared to other subduction zones in the world and is most likely due to the morphology of the Cocos plate.

The seismic environment of Mexico is summarized in these three large groups, and is represented through a model of seismic sources, shown in **FIGURE 9**, some of the seismic sources are modeled as area type and others as *rectangular fault*[3]. The boundaries of these seismic sources are defined based on different criteria, such as geological faults, distribution of the seismic catalog, mechanisms of fault, previous zoning, among others. For this case, we used a seismic catalog made up of various sources of information [**10**]–[**12**], which covers a time window since 1900 with thousands of records. **FIGURE 10** shows the spatial distribution of this catalog in the vicinity of the pipeline.

It is usually impossible to determine the seismic hazard by simply counting the number of times given values of intensity have been exceeded at the site in question. This is because a complete catalog of the accelerations that have occurred at such a site is rarely available. It is therefore necessary to calculate the seismic hazard under a probabilistic approach using statistical processes to quantify and consider the uncertainties that the phenomenon itself represents.

In this case, the modified Gutenberg-Richter [**13**] and Characteristic Earthquake (CE) [**14**] seismicity models were used. The determination of the parameters that define each of the seismicity models is made by means of statistical processes that consider the completeness and duration of historical catalogs of earthquakes [**15**]–[**18**].

[2] MMIS: The Modified Mercalli Intensity Scale | U.S. Geological Survey (usgs.gov)

[3] Rectangular fault: type of seismic source available in R-CRISIS program

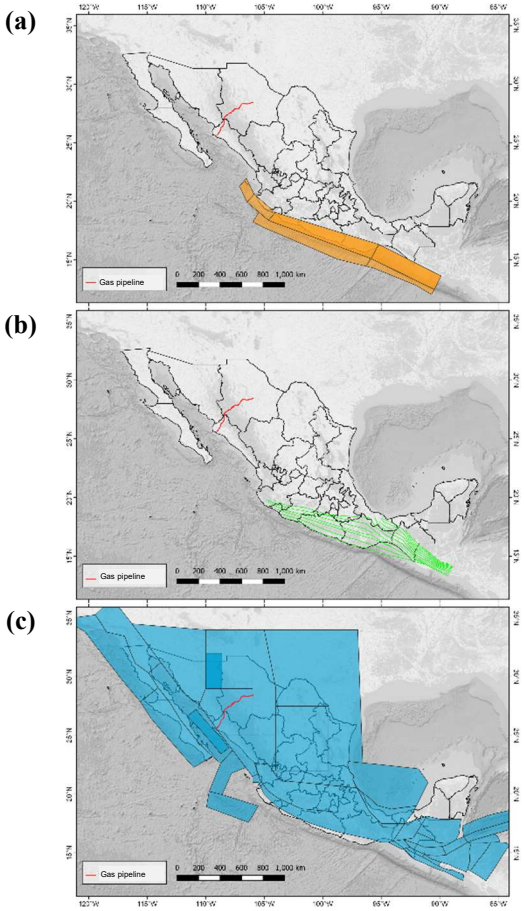

FIGURE 9: SEISMIC SOURCES: A) SUBDUCTION, B) INTERMEDIATE DEPTH, C) CORTICAL (GAS PIPELINE IS SHOWN WITH A RED LINE)

Once the activity rate of each of the seismic sources is determined, it is necessary to evaluate the effects each of them produces at a site of interest, in terms of seismic intensity (e.g., acceleration, velocity or displacement). To do this, it is necessary to know the intensity that would be present at the site in question if an earthquake with a given magnitude were to occur at the *i-th* source. The relationships between magnitude, relative source-site position and intensity are known as attenuation models (or GMPMs).

Attenuation models are selected based on the type of faulting (mechanism of fault) characteristic of each seismic source. In some cases, it is possible to use local models, (i.e., built from events specific to the source). However, in other cases there is not enough information to build local models, so models from other similar tectonic environments are used. Some of the attenuation models used to calculate the seismic hazard in Mexico are described in [**19**]–[**23**].

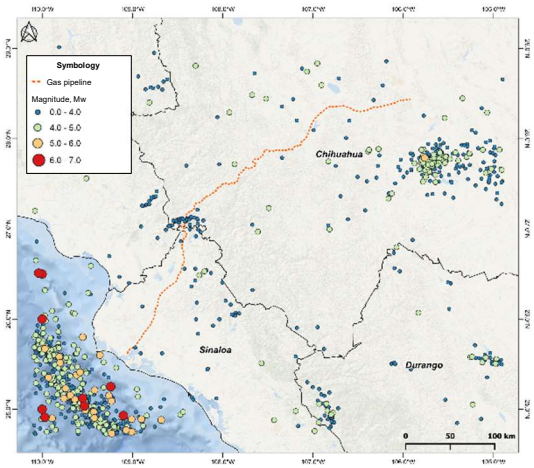

FIGURE 10: SEISMIC CATALOG 1900-2020 IN THE TOPOLOBAMPO PIPELINE AREA (PIPELINE IS SHOWN WITH A RED LINE)

Once the seismicity of the sources and the attenuation patterns of the waves generated in each of them are known, the seismic hazard can be calculated using the following expression proposed by [**24**], [**25**].

$$v(Sa) = \sum_{i=1}^{N} \int_{M_0}^{M_{ui}} -\frac{d\lambda_i(M)}{dM} Pr(SA > Sa|M, R_i) dM \qquad \textbf{(1)}$$

Where:

$\sum(\cdot)$ - sum and covers the totality of the seismic sources, N,
$Pr(SA > Sa|M, R_i)$ - probability that the intensity exceeds a certain value, given the magnitude of the earthquake, M, and the distance between the *i-th* source and the site, R_i.

The probability is calculated as shown in Equation **(2)**, given the magnitude and distance, assuming that the intensity has lognormal distribution.

$$Pr(SA > Sa|M, R_i) = \Phi\left(\frac{E(\ln S\,a|M, R_i) - \ln S\,a}{\sigma_{\ln Sa}}\right) \qquad \textbf{(2)}$$

With $\Phi(\cdot)$ being the standard normal distribution.

The seismic hazard assessment was carried out in R-CRISIS V20.3, an open-source software developed by [**26**]. Peak ground acceleration (PGA) results were obtained for different return periods: 20, 50, 100, 250, 500 and 1,000 years. In all cases, the same pattern was observed, with maximum values occurring near the Pacific coast and minimum values in the interior of the continent. This is consistent with the seismicity of the area and the distribution of historical earthquakes. As an example, the

accelerations obtained for the 500-year return period are presented in **FIGURE 11**.

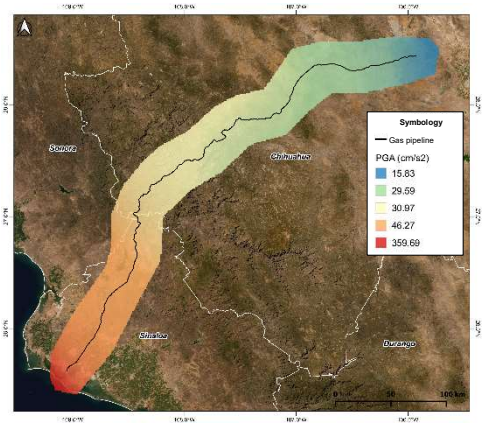

FIGURE 11: PEAK GROUND ACCELERATION (PGA) FOR 500 YEARS RETURN PERIOD

2.5 Landslide Hazard Assessment

Mass removal processes (MRP) occur in mountainous areas where several elements favor their occurrence, such as unfavorable lithologies, steep relief, tectonic effects, humid climates, and associated seismicity. The methodology proposed in this work is limited only to flat or translational landslides, since the other movement mechanisms are controlled by very particular geotechnical and geological-structural characteristics, making it impossible to consider them in a regional analysis.

2.5.1 Landslide due to earthquakes

In translational sliding, the mass of material moves downward along a flat or slightly undulating surface and has little or no rotational or overturning motion. Translational movements are frequent in rock zones affected by discontinuities, (e.g. fractures, folding, shearing), with an orientation relatively parallel to the slope, as well as on slopes whit a considerable thickness of soil or detrital material in contact with a zone of less altered rock. This condition, although not the only one, prevails in many real cases where a weathered layer of soil or rock lies on top of more competent strata, creating a contact surface that functions as a sliding surface.

It is common in engineering to define slope stability in terms of a factor of safety (FS), obtained from a mathematical stability analysis. Not all factors affecting slope stability can be quantified for inclusion in a mathematical model, such as slope geometry, geological parameters, presence of tension cracks, dynamic loads due to seismic action, water flow, and material properties. Despite the weaknesses, the FS is a useful tool for decision making.

In general terms, the definition of FS is the ratio between the resisting forces F_{res} (which oppose slip) and the acting forces F_{act} (which induce slip).

$$FS = \frac{F_{res}}{F_{act}} \quad \textbf{(3)}$$

Expressed in terms of stress, it would be as follows.

$$FS = \frac{\tau_{res}}{\tau_{act}} \quad \textbf{(4)}$$

Where:

τ_{res} – resisting stress, and
τ_{act} - acting stress

Stability analyses are intended to give a quantitative idea of the degree of safety of a slope. FS values less than one indicate instability, values greater than one indicate stability and a value of one indicates a limit equilibrium state.

For a uniform and relatively long slope, where edge effects are negligible, the factor of safety can be calculated for an infinite slope of one unit area, using the Mohr - Coulomb criterion. The basic equation for determining the shear resistance can be represented by the Mohr-Coulomb equation [**27**]:

$$\tau_p = c + \sigma_n \tan\phi \quad \textbf{(5)}$$

Where:

c - cohesive strength of the cemented surface
ϕ - friction angle
τ_p - maximum value of shear strength, and
σ_n - normal stress

Therefore, it is necessary to adapt this concept of the two-dimensional infinite slope within the analyses that can be carried out with the help of Geographic Information Systems, to make regional estimates.

In conditions where there is a fault parallel to the slope surface, at a certain depth and the length of the fault is long compared to its thickness, the infinite slope analysis can be used as an approximation (**FIGURE 12**).

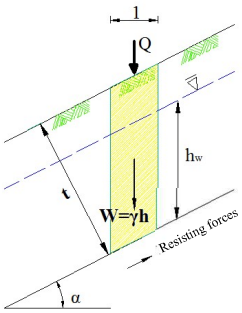

FIGURE 12: SIMPLIFIED SCHEME OF THE INFINITE SLOPE METHOD

There are several ways to express the factor of safety, but one that is easy to handle is [**28**].

$$FS = \frac{c'}{\gamma \cdot t \cdot \sin\alpha} + \frac{\tan\varphi'}{\tan\alpha} - \frac{m \cdot \gamma_w \cdot \tan\varphi'}{\gamma \cdot \tan\alpha} \qquad \textbf{(6)}$$

Where:

ϕ' - effective friction angle
c' - effective cohesion
α - slope angle
γ - specific weight of the material
γ_w - specific weight of water
t - material thickness, measured perpendicular to the failure plane, and
m - proportion of the material thickness that is saturated

This equation is divided into three terms, the first is the cohesive component of the resistance, the second is the frictional component and the third term considers the decrease in resistance due to pore pressure.

It should be noted that the thickness, t, is measured perpendicular to the slip plane, unlike other expressions where the vertical distance is used.

In general, to model the dynamic response of slopes, the method of permanent displacements developed by [**29**] can be used. This work consists of modeling a landslide as a rigid, frictional block on an inclined plane (**FIGURE 13**). The block has a critical acceleration, a_c, which represents the acceleration threshold required to overcome the shear resistance and promote sliding.

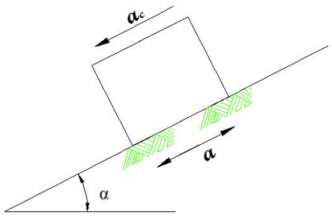

FIGURE 13: DIAGRAM OF INCLINED BLOCK IN NEWMARK ANALYSIS

The critical acceleration is a function of the static factor of safety and the slip geometry. It can be expressed as:

$$a_c = (FS - 1)\sin\alpha \qquad \textbf{(7)}$$

Where:

a_c - critical acceleration (in terms of g, the acceleration of gravity)
FS - factor of safety under static conditions, and
α - slope angle.

The angle α in this case, refers to the direction in which the center of gravity of the mass moves when sliding occurs. In regional scale analysis, the value of the thrust angle is practically equal to the slope angle of the slopes.

To apply the Newmark method in regional landslide analysis in Mexico, [**1**], [**2**] developed a simplified procedure that incorporates an empirical equation to estimate the Newmark displacement, D_N, as a function of the earthquake intensity and the critical acceleration, a_c, for subduction earthquakes (Equation **(8)**) and normal fault earthquakes (Equation **(9)**). D_N is the displacement in centimeters, a_c is the critical acceleration and a_{max} is the maximum ground acceleration [**30**], [**31**]. These same authors consider $D_N = 5\ cm$ as a critical value, which characterizes the failure of a slope and promotes its sliding. This conservative value represents slopes formed by brittle rocks [**32**]. The D_N value of 5-10 cm is a critical value for failure in silty-clay slopes, and 10 cm for slopes formed by cohesive soils [**33**].

In summary, D_N values within the range of 5-10 cm increase the probability of slope failure, as summarized in **TABLE 1**.

TABLE 1: RANGE OF D_N VALUES THAT INCREASE THE PROBABILITY OF SLOPE FAILURE

Newmark displacement	Affected materials
5 cm	Fragile rocks
5-10 cm	Silty-clay materials
10 cm	Clay materials

The general methodology for generating an earthquake-induced landslide map is explained in **FIGURE 14**.

$$\log D_N = -1.2841 + \log\left[\left(1-\frac{a_c}{a_{max}}\right)^{1.9518}\left(\frac{a_c}{a_{max}}\right)^{-1.2786}\right] \pm 0.5882 \quad \textbf{(8)}$$

$$\log D_N = -0.7819 + \log\left[\left(1-\frac{a_c}{a_{max}}\right)^{2.2627}\left(\frac{a_c}{a_{max}}\right)^{-1.3779}\right] \pm 0.7351 \quad \textbf{(9)}$$

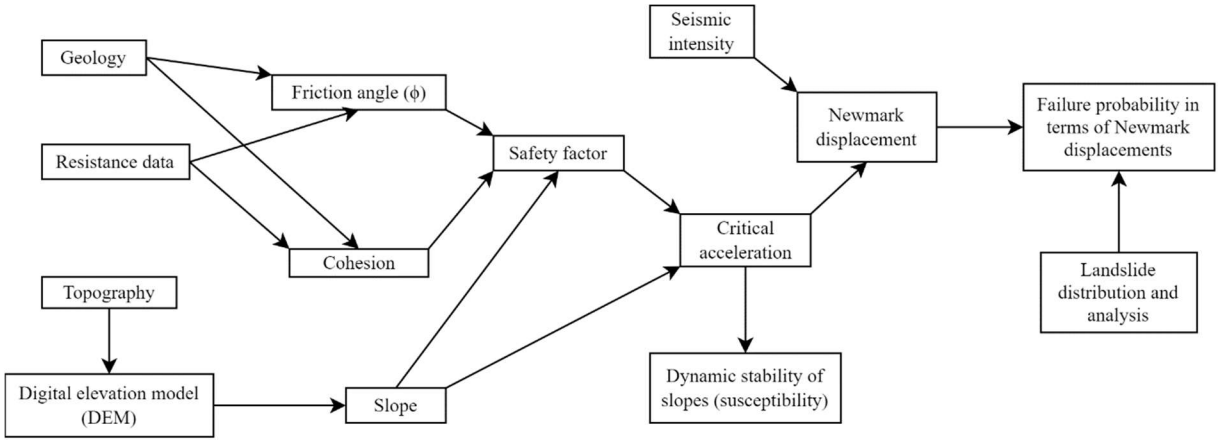

FIGURE 14: FLOWCHART TO GENERATE A MAP FOR SEISMICALLY INDUCED LANDSLIDES

2.5.2 Landslide due to rainfall

Earthquakes represent an important percentage in the occurrence of landslides, but the statistics of landslides around the world show that rainfall causes an even greater number of this type of events.

Continuing with the concept of the infinite slope, researchers such as [**2**], [**34**] have proposed expressions to evaluate the terrain conditions under which it will tend to move. For this purpose, they define a parameter called steady-state critical precipitation, Q_c, which is the precipitation necessary for a landslide to occur in a terrain with defined characteristics.

$$Q_c = \frac{T \cdot \sin\alpha}{a/b}\left[\frac{c'}{\rho_w \cdot g \cdot h \cdot \cos^2\alpha \cdot \tan\phi} + \frac{\rho}{\rho_w}\left(1-\frac{\tan\alpha}{\tan\phi}\right)\right] \quad \textbf{(10)}$$

Where:

T - transmissivity of the soil along its thickness
ρ - density of the material
ρ_w - density of water
a - tributary area uphill
b - length of the sliding terrain

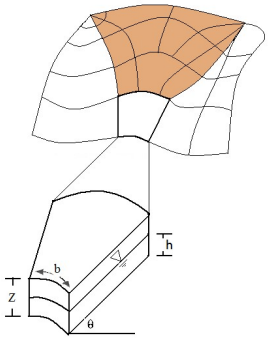

FIGURE 15: ILLUSTRATION OF THE PARAMETERS USED IN EQUATION **(10)**

For the case of soils where the material does not present cohesion, Equation **(10)** is considerably simplified, as shown in Equation **(11)**

$$Q_c = \frac{T \cdot \sin\alpha}{a/b}\left[\frac{\rho}{\rho_w}\left(1 - \frac{\tan\alpha}{\tan\phi}\right)\right] \quad \textbf{(11)}$$

Cases may occur where precipitation will not affect the behavior of the terrain, known as unconditionally stable slopes, which can be evaluated as:

$$\tan\alpha < \frac{c'}{\rho \cdot g \cdot h \cdot \cos^2\alpha} + \left(1 - \frac{\rho}{\rho_w}\right)\tan\phi \quad \textbf{(12)}$$

The opposite case will be the one where material sliding is imminent due to a very steep slope, this condition is defined as unconditionally unstable slopes, which is evaluated as follows:

$$\tan\alpha > \tan\phi + \frac{c'}{\rho \cdot g \cdot h \cdot \cos^2\alpha} \quad \textbf{(13)}$$

Likewise, the methodology described above for earthquakes can be used, adapted to the case of rainfall. In this case, the procedure is the same, using Equations **(10)** and **(11)** to define the critical precipitation, Q_c, instead of the critical acceleration, a_c.

Following the methodologies described above, the values of critical acceleration, a_c, and critical precipitation, Q_c, were obtained. These values are specific to the study area, i.e., they depend exclusively on soil properties and topography; in terms of Equation **(3)**, they would be the forces opposing sliding, F_{res}. On the other hand, the forces inducing the landslide, F_{act}, were characterized from a probabilistic point of view, which represents an added value for the calculation methodology since all possible scenarios are being considered, each one weighted by its occurrence rate. These intensities would correspond to the maximum accelerations and precipitation, a_{max} and Q_{max}, respectively.

Subsequently, the ratios a_{max}/a_c and Q_{max}/Q_c were determined for which there would be three possible scenarios:

<1.0: the safe state, (the soil offers sufficient resistance so that a landslide would not be detonated)

=1.0: full equilibrium, ($F_{act} = F_{res}$) and

>1.0: instability, (there is susceptibility to soil sliding).

It is important to mention that these scenarios arise from the interpretation of the quotient between F_{act} and F_{res}, however, behind them there are sources of uncertainty that are impossible to remove. For this reason, the previously described thresholds may be modified, up or down, at the analyst's discretion to capture these sources of variation.

Whole methodologies described in the previous sections were integrated into routines developed in Visual Basic .NET [**8**] and SIG software [**6**].

3. RESULTS AND DISCUSSION

For landslides triggered by earthquakes, two interesting results were obtained: In Sinaloa results indicate high PGA (a_{max}) values, the terrain presents small slopes and competent soil conditions, therefore the critical acceleration, a_c, necessary to initiate a landslide should be extremely high. As a result, there is no hazard associated because an excessively high critical acceleration (a_c), related to a very high returned period should be needed. For Chihuahua section, PGA (a_{max}) values are considerably lower, the topography and soil characteristics show that a_c needed is much lower to initiate a landslide, therefore there is neither a hazard associated, but this zone requires further attention as any reduction in the value of a_c would result in changes of susceptibility to landslides. This condition can be easily controlled by using proper mitigation structures like trench and slopes breakers, which is a construction technique widely used as a geotechnical remediation measure in the pipeline right of way

For landslides triggered by rain and based to historical records, precipitation rates are high, therefore, during the analysis, soil was assumed to be saturated. Results for Sinaloa indicated low hazard due to topography and soil conditions consisting of small slopes and competent soil, therefore an excessively high critical rainfall (Q_c) and return period should be needed to initiate a slippage. For Sierra Madre Occidental area, Q_c is considerably less due to the topography (high slope gradients) and soil conditions; Therefore some zones of interested were identified, which ones have been properly managed not only during construction where mitigation structures (slope breakers **FIGURE 16**.) were installed; but also during operations where continue monitor activities are part of the integrity program.

The assessment results allowed to identify zones of interest along Topolobampo pipeline, which were site inspected with TC Energy team, to compare the probabilistic model results with current field conditions. It was possible to corroborate that the zones of interest resulted from the probabilistic slippage analysis, were identified during project construction and are managed trough integrity program

Mitigations structures where no considered at the first analysis and landslide models, but one of the advantages of the methodology implemented, is to allow updating any of the calculation variables, such as the effect of these ground structures. This allows refining the calculations based on current conditions or changes performed during the lifetime of the system. By making this modification to the DEM, runoff velocities and flood flow rates decreased considerably.

FIGURE 16: PRESENCE OF STREAM CUTTERS IN RIGHT OF WAY

4. CONCLUSIONS

From the studies carried out during the pipeline engineering design and construction, it was possible to extract valuable soil information from almost 100 geotechnical boreholes, which were used to create a GIS database covering the entire system alignment.

Based on the information available for the area, it was possible to characterize the precipitation and seismic hazards. In both cases, a probabilistic approach was used in which a statistical treatment of the data and a correct handling of uncertainties were carried out. As a result, precipitation and PGA values were obtained for different return periods.

From the analyses, it was concluded that the seismic-triggered landslide hazard has a low effect along the entire length of the pipeline. Despite the variability of the triggering phenomenon and soil properties, the assessment shows that the importance remains on the interaction of these factors: Simply having a high accelerations does not mean that the zone is prone to landslides; likewise, despite the fact that the soil presents low resistance levels, the susceptibility to landslides will be low if there is no triggering phenomenon present.

From assessment results, some zones of interest were found, which matched with areas already being monitored through the pipeline integrity program or already had a mitigation structure.

Consistency was found between the models and the conditions observed along the pipeline, showing that validation is important to calibrate the models to maximize certainty in the results.

The study demonstrated how mitigation and prevention can be incorporated into the models to best represent the current pipeline site condition.

The zones of interest identified in the study represent only zones with hazards related to geological and hydrological behavior. However, to perform a complete integrity analysis that identifies the impact on the pipeline, it is necessary to take into account the mechanical stress and operating conditions of the pipeline, applying other widely known methodologies and analyses that are out of the scope of this paper.

ACKNOWLEDGEMENTS

Special thanks to the TC Energy team for giving us the opportunity to present the results of the landslide hazard assessment for Topolobampo pipeline. Likewise, thanks to operations team for their support during the visits made to the project.

We also grateful to SÍSÉ Salud Estructural and AON- ERN team for their valuable contribution with the methodologies and tools used for the evaluation and execution of this study, as well as their availability during the execution of the project to comply with the safety requirements that are key part of TC Energy values.

REFERENCES

[1] M. Niño, M. A. Jaimes, and E. Reinoso, “Seismic-event-based methodology to obtain earthquake-induced translational landslide regional hazard maps,” *Natural Hazards*, vol. 73, no. 3, pp. 1697–1713, Sep. 2014, doi: 10.1007/s11069-014-1163-y.

[2] M. A. Jaimes, M. Niño, and B. Huerta, “Hurricane event-based method to create regional hazard maps for heavy rainfall-induced translational landslides,” *Natural Hazards*, vol. 76, no. 2, pp. 1143–1161, Mar. 2015, doi: 10.1007/s11069-014-1539-z.

[3] TC Energía, “Sistema El Encino — Mazatlán,” *Activos*, 2023. https://www.tcenergia.com/activos/sistema-el-encino--mazatlan/

[4] B. Lehner, K. Verdin, and A. Jarvis, “New Global Hydrography Derived From Spaceborne Elevation

Data," *Eos, Transactions American Geophysical Union*, vol. 89, no. 10, p. 93, Mar. 2008, doi: 10.1029/2008EO100001.

[5] T. G. Farr *et al.*, "The Shuttle Radar Topography Mission," *Reviews of Geophysics*, vol. 45, no. 2, p. RG2004, May 2007, doi: 10.1029/2005RG000183.

[6] QGIS Development Team, "QGIS Geographic Information System." [Online]. Available: https://www.qgis.org

[7] TransCanada, "TEP-IN-WOF-GL Weather and Outside Forces Threat Management (CAN-US-MEX)," 2018.

[8] F. Balena and J. Fawcette, *Programming Microsoft Visual Basic 6.0*, vol. 1. Microsoft press Washington, 1999.

[9] S. K. Singh, G. Suárez, and T. Dominguez, "The Oaxaca, México earthquake of 1931: Lithospheric normal faulting in subducted Cocos plate," *Nature*, vol. 317, pp. 56–58, 1985.

[10] G. Ekström, M. Nettles, and A. M. Dziewoński, "The global CMT project 2004–2010: Centroid-moment tensors for 13,017 earthquakes," *Physics of the Earth and Planetary Interiors*, vol. 200–201, pp. 1–9, Jun. 2012, doi: 10.1016/j.pepi.2012.04.002.

[11] D. A. Storchak *et al.*, "Public Release of the ISC-GEM Global Instrumental Earthquake Catalogue (1900-2009)," *Seismological Research Letters*, vol. 84, no. 5, pp. 810–815, Sep. 2013, doi: 10.1785/0220130034.

[12] I. de G. Universidad Nacional Autónoma de México, "Servicio Sismológico Nacional, México," 2020. http://www.ssn.unam.mx

[13] C. A. Cornell and E. H. Vanmarcke, "The Major Influences on Seismic Risk," in *Proc. of the 4th World Conference on Earthquake Engineering*, Santiago de Chile, Chile, 1969, pp. 69–83.

[14] R. R. Youngs and K. J. Coppersmith, "Implications of fault slip rates and earthquake recurrence models to probabilistic seismic hazard estimates," *Bulletin of the Seismological Society of America*, vol. 75, no. 4, pp. 939–964, 1985.

[15] M. G. Ordaz and S. Giraldo, "Joint Maximum Likelihood Estimators for Gutenberg-Richter Parameters λ 0 and β Using Subcatalogs," *Earthquake Spectra*, vol. 34, no. 1, pp. 301–312, 2018, doi: 10.1193/092816EQS162M.

[16] J. Arboleda and M. G. Ordaz, "Un mejor uso de los datos estadísticos para estimación de la sismicidad local," in *Memoria del X Congreso Nacional de Ingeniería Sísmica*, Puerto Vallarta, México: Sociedad Mexicana de Ingeniería Sísmica, A.C., 1993, pp. 21–27.

[17] A. Kijko and A. Smit, "Extension of the Aki-Utsu b-Value estimator for incomplete catalogs," *Bulletin of the Seismological Society of America*, vol. V 102, no. No. 3, pp. 1283–1287, 2012, doi: 10.1785/0120110226.

[18] A. Kijko, "Estimation of the maximum earthquake magnitude, Mmax," *Pure Appl Geophys*, vol. V161, pp. 1–27, 2004.

[19] N. A. Abrahamson, W. J. Silva, and R. Kamai, "Summary of the ASK14 Ground-Motion Relation for Active Crustal Regions," *Earthquake Spectra*, vol. 30, no. 3, pp. 1025–1055, 2014, doi: 10.1193/070913EQS198M.

[20] B. S.-J. Chiou and R. R. Youngs, "Update of the Chiou and Youngs NGA Model for the Average Horizontal Component of Peak Ground Motion and Response Spectra," *Earthquake Spectra*, vol. 30, no. 3, pp. 1117–1153, 2014, doi: 10.1193/072813EQS219M.

[21] M. A. Jaimes, A. Ramirez-Gaytan, and E. Reinoso, "Ground-Motion Prediction Model from Intermediate-Depth Intraslab Earthquakes at the Hill and Lake-Bed Zones of Mexico City," *Journal of Earthquake Engineering*, vol. 19, no. 8, pp. 1260–1278, 2015, doi: 10.1080/13632469.2015.1025926.

[22] J. C. Reyes, "El estado límite de servicio en el diseño sísmico de edificios," Tesis de Doctorado, Facultad de Ingeniería. Universidad Nacional Autónoma de México. Febrero., 1999.

[23] J. X. Zhao *et al.*, "Attenuation relations of strong ground motion in Japan using site classification based on predominant period," *Bulletin of the Seismological Society of America*, vol. 96, no. 3, pp. 898–913, 2006, doi: 10.1785/0120050122.

[24] L. Esteva, "Criterios para la construcción de espectros para diseño sísmico," in *3er Simposio Panamericano de Estructuras*, Caracas, Venezuela, 1967.

[25] C. A. Cornell, "Engineering seismic risk analysis," *Bulletin of the Seismological Society of America*, vol. 58, no. 5, pp. 1583–1606, 1968.

[26] M. G. Ordaz, F. Martinelli, A. Aguilar, J. Arboleda, C. Meletti, and V. D'Amico, "R-CRISIS Ver 20.3.0 (Core library 20.3.0.0)." Program for computing seismic hazard, 2023. [Online]. Available: http://www.r-crisis.com/

[27] E. Hoek and J. W. Bray, *Rock Slope Engineering, Institution of Mining and Metallurgy*, 3ra ed. 1996.

[28] R. W. Jibson, E. L. Harp, and J. A. Michael, "A method for producing digital probabilistic seismic landslide hazard maps," *Eng Geol*, vol. 58, pp. 271–289, 2000.

[29] N. M. Newmark, "Effects of earthquakes on dams and embankments," *Geotechnique*, vol. 15, pp. 137–160, 1965.

[30] R. W. Jibson, "Regression models for estimating coseismic landslide displacement," *Eng Geol*, vol. 91, pp. 209–218, 2007.

[31] N. N. Ambraseys and J. M. Menu, "Earthquake-induced ground displacements," *Earthq Eng Struct Dyn*, vol. 16, pp. 985–1006, 1998.

[32] R. Romeo, "Seismically induced landslide displacements: a predictive model," *Eng Geol*, vol. 58, no. 3–4, pp. 337–351, 2000.

[33] R. W. Jibson and D. K. Keefer, "Analysis of the seismic origin of landslides: examples from the New Madrid seismic zone," *Geol Soc Am Bull*, vol. 105, pp. 521–536, 1993.

[34] D. R. Montgomery, K. Sullivan, and H. M. Greenber, "Regional test of a model for shallow landsliding," *Hydrol Process*, vol. 12, pp. 943–955, 1998.